2012 International Conference on Geological and Environmental Sciences
IPCBEE vol.36(2012) © (2012)IACSIT Press, Singapoore

Land Coverage Changes in the Hulun Buir Grassland of China Based on the Cellular Automata-Markov Model

Du Huishi, Hasi Eerdun[+] , Yang Yi, and An Jing

College of Resources Science and Technology, Beijing Normal University, Beijing 100875, China

Abstract. This study aims to investigate the land coverage change in Hulun Buir Grassland of China. The land coverage changes for the past 50 years in a typical region of the Hulun Buir Grassland were interpreted and analyzed. A series of remote sensing data (Aerial photo or QuickBird) in 1959, 2002, 2004, and 2009 were used to extract the information. Future land coverage scenarios were simulated by integrating the Markov process into the cellular automata model. The results showed that all land use types had large variable amplitudes. The grassland area decreased, whereas other areas increased. The areas of flowing blowouts and depositional regions decreased by 71 340.80 and 867 777.60 m^2, respectively, because artificial sand fixation over the past five years. The predicted land coverage pattern kept current development trend for 2012–2020, while the growth rate decreased. The amplitudes of flowing blowouts and depositional regions increased by 27.10% and 10.13%, respectively. In contrast, the development pace significantly decreased. The amplitudes of fixed blowouts and depositional areas increased by 59.04% and 41.44%, respectively.

Keywords: land coverage, cellular automata–Markov model, Hulun Buir

1. Introduction

Land use and cover change (LUCC) are among the most important alterations of the Earth's land surface (Lambin et al., 2001). And it contributes to the global changes and constitutes the essential reasons for that. Nowadays, LUCC and landscape transformation processes have accelerated in China. Consequently, understanding and predicting the causes, processes and consequences of LUCC has become a major challenge to anyone involved in landscape ecology, regional land coverage change planning, biodiversity conservation, and control desertification (Etter, et al., 2006; Wang et al., 2012). LUCC is a complex process subject to the interactions between natural and social systems on different temporal and spatial scales (Veldkamp and Lambin, 2001). And accurate methods of land coverage change assessment have been developed, and are currently used, by the scientific community. The detection of land use change using remote sensing and GIS software is a "hotspot" and important study field (Cheema and Bastiaanssen, 2010). There are numerous studies on Land coverage change and its dynamic simulation (Xiao et al., 1991; Tang et al., 2010).

Dune blowouts, consisting of erosional saucers, bowls, troughs, and other morphological forms, are the most common erosional dune form in coastal, semi-arid, and desert environments (Hesp, 2002). In China, blowouts are mainly distributed in sandy land and desert regions such as Hulun Buir, Hunshadake, and Kerqin. The Hulun Buir Grassland is a part of the European-Asian grassland of central Asia. This grassland is one of the best maintained in China. Unfortunately, aeolian action is destroying this grassland. Therefore, the morphological evolution of the blowouts in this region urgently needs to be studied.

Land surface digital simulation aids the inversion of the historical process and the prediction of future changes (Andreas and Joanna, 2010). The CA-Markov model is advantageous. Long-term predictions can be made, and the spatial changes of complex systems can be simulated with more accuracy and practicality. The

[+] Corresponding author. Tel.: + (8613910411308); fax: +(8601058805423).
E-mail address: (hasi@bnu.edu.cn).

paper simulated land cove change in the Hulun Buir Grassland using the 3S platform and the CA-Markov Model. The findings are significant in controlling desertification, enriching the study of aeolian landforms.

2. General situation and data processing of the study area

The study area (49 km^2) is located at the juncture region between Hailaer City (Inner Mongolia) and the Chenbaerhu flag (119°35′49″ to 119°42′36″ E and 49°13′30″ to 49°16′56″ N). The area is flat sandy grassland on the eastern margin of the Hailaer Sand Belt and south of the Hailaer River. With gentle topographic relief, the area is a typical high plain and has a temperate continental monsoon climate. The average annual temperature, rainfall, wind speed, and gale times are -1.3 °C, 353.7 mm, 3.2 $m \cdot s^{-1}$, and 20 d to 40 d, respectively.

The remote sensing data used included aerial photographs taken in 1959, clean sky QuickBird images taken on August 2002, May 2004, and April 2009, 1:10 000 topographic maps, meteorological data, a statistical yearbook, among others. Remote sensing data were pre-treated as follow: (1) bands compositing; (2) ground control points selection by RTK GPS in study region; (3) geometric precise correcting (the error was less than 2 pixels). To improve precision, the multiplied standard deviation tension method was used to interpret blowouts and deposition regions.

The study area was divided into 10 land coverage types, namely, cultivated land, forestland, grassland, water area, building site, flat sandy land, fixed blowout, fixed depositional region, flowing blowout, and flowing depositional region. To improve classification precision, various information pieces were extracted using the GIS software with a man-machine interactive interpretation based on knowledge. After comparison and analysis, minimum map patches within 6 pixels were controlled in the interpretation to consider the influence of spatial scale.

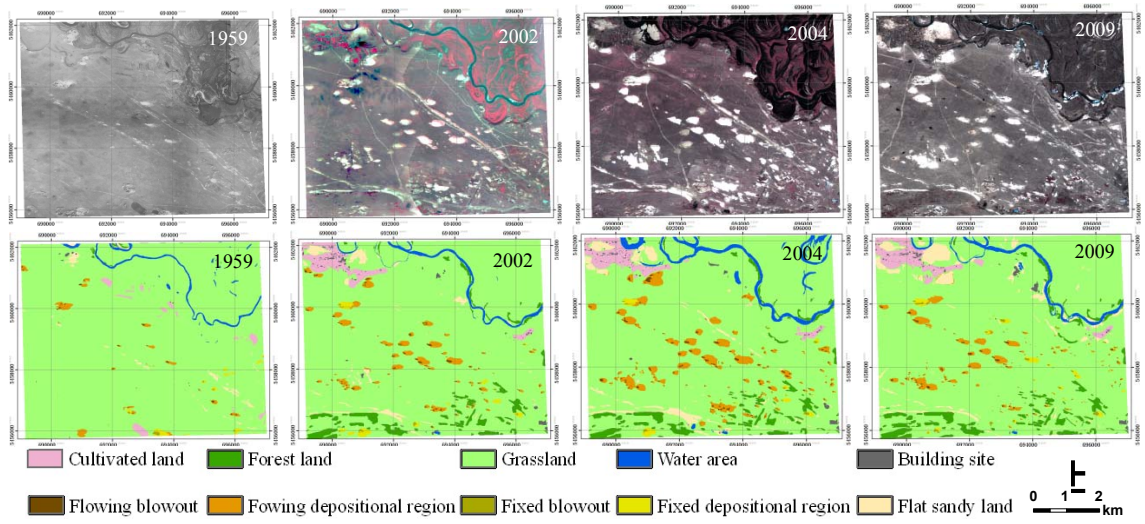

Fig. 1 Aerial photo, QuickBird false color image, and interpretation graphs

3. Method

3.1. Markov model

If the random process belongs to the finite sequential $t_1<t_2<t_3 \ldots t_n$, the arbitrary status a_n at arbitrary moment t_n is only related to the status a_{n-1} at the former moment t_{n-1}. The process having the Markov property was named as the Markov process. For the variation predictions, the land use/cover change process was treated as the Markov process. The land use type in a certain period corresponds to the possible state in the Markov Model. A prediction can be made using the following equation:

$$S_{(t+1)}=P_{ij} \times S_{(t)} \quad (1)$$

where $S_{(t)}$ and $S_{(t+1)}$ are respectively the states of land use type. At the moment t and t+1, P_{ij} is the state transition matrix.

3.2. CA model

The characteristics of the CA Model are time, space, and discrete state. Every variable only has a finite number of states, and the rules of state changes are manifested as local characteristics. The CA Model can be expressed as the following equation:

$$S_{(t+1)} = f(S_{(t)}, N) \quad (2)$$

where S is the cellular finite discrete state set, t and t+1 are the mean different moments, and f is the cellular transformation rule in local space.

3.3. CA-Markov model

According to the characteristics of the individual CA and Markov models, they can be combined with each other. The study area was divided into several sections, and each section is a cellular one. Each cellular section has a corresponding state and neighbors. The present states of the cellular and neighboring sections determine the future state. Each pixel is a cellular section in raster maps, and each cellular land use type is its state. The specific realization processes are as follow: (1) Determination of conversion rules. By converting interpreted data from vector to raster, via a GIS overlay analysis, the transition probability matrix as well as transition and conditional probability images of land use types can be determined. (2) Construction of CA filters. Weight factors with remarkable spatial significance are created based on the distance between the cellular and neighboring sections. The cellular change of state is then determined. A 5 × 5 filter is used, meaning a rectangular space that is composed with one cellular section. This filter has a remarkable influence on the change in the cellular state. (3) Determination of start time and iteration number. Based on the land use pattern in 2002, the CA cycle number is chosen, and the land use pattern of 2009 is simulated to test the simulation accuracy. The future state can be predicted according to the practical land use pattern of 2009. There are many simulation platform can run it, such as the Geographical Simulation and Optimization System (http://www.geosimulation.cn/index_chs.html), Dinamica EGO (http://www.csr.ufmg.br/dinamica/index.html), and Idrisi software. We used Idrisi Taiga edition in this paper.

4. Results and analysis

4.1. Structural changes in land coverage

The forestland area had the highest amplitude increase, mainly because of a plantation in the extended aeolian region (Table 1). The water area gradually increased and reached its highest value in 2004. This peak value can be attributed to the amount of rainfall in 2004 and the large area of the Oxbow Lake. Owing to population increase and rapid economy development, the average annual growth rates of cultivated lands and building sites are 4.04% and 17.84%. The areas of flowing blowouts and depositional regions initially increased, and then decreased, especially in the past five years. After re-vegetating the forest and using an artificial grass square grid to fix sand, the areas of the abovementioned flowing sections decreased to 71 341 and 867 7788 m^2, respectively. The areas of fixed blowouts and depositional regions increased to 58 459 and 58 475 m^2 in the past five years. The areas of flat sandy lands that used to be a vehicle lane and a discarded building land continuously increased. The annual average increase was 7.59%. The main landscape type in this section is grassland, from which other land coverage types are increasingly being transformed.

Table 1 Changes in land coverage types from 1959 to 2009 (m^2)

	Cultivated land	Forestland	Grassland	Water area	Building site	Flowing blowout	Flowing depositional region	Fixed blowout	Fixed depositional region	Flat sandy land
1959	455 104	56 405	47 192 423	648 920	24 677	50 060	395 932	35 030	196 445	380 389
2002	1 274 664	1 754 169	42 948 702	654 970	224 393	157 607	1 172 670	64 825	217 154	966 231
2004	1 315 286	1 820 460	41 363 959	1 016 179	227 839	224 790	2 036 245	65 161	220 174	1 145 292
2009	1 374 772	2 094 378	41 303 726	873 603	244 798	153 449	1 168 467	123 620	278 649	1 819 923
Area change	919 668	2 037 973	-5 888 697	224 683	220 121	103 389	772 535	88 590	82 204	1 439 534
Change range	202.08	3 613.11	-12.48	34.62	892.01	206.53	195.12	252.90	41.85	378.44

Within the study period, after the original cultivated land was abandoned, it was recovered and became grassland (Table 2). Some areas were fixed after wind erosion. Some areas became building lands. Original forestlands with a smaller distribution degenerated into grasslands. Small forestlands around rivers turned into water and flat sandy lands. Grasslands were the source of many other land use types. As a result of wind erosion, some areas formed forestlands, fixed blowouts, and fixed depositional regions by artificial action.

Grasslands were also the main source of cultivated and building lands. Water was mainly transformed into grasslands, forestlands, or flat sandy lands and these transformations were primarily caused by river swinging, increased river area, and grassland erosion on both river sides. Building land was mainly transformed from grasslands and forestlands. Flowing blowouts were mainly transformed from eroded grasslands and vehicle lanes. Grassland transformations accounted for 32.46% of the grassland area. Grasslands were also transformed from activated original fixed blowouts and depositional regions. The flowing depositional region was related to the flowing blowout. After wind-eroded sand materials accumulated in poster lateral blowouts, the original grassland was covered. Fixed blowouts and depositional regions were formed from the original blowout fixation, grasslands, and some parts of forestlands. Flat sandy lands mainly transformed from grasslands and forestlands.

Table 2 Transition probability matrix of land coverage types from 1959 to 2009 (%)

	Cultivated land	Forestland	Grassland	Water area	Building site	Flowing blowout	Flowing depositional region	Fixed blowout	Fixed depositional region	Flat sandy land
Cultivated land	2.93	3.53	91.40	0.00	0.95	0.00	0.00	1.02	0.00	0.18
Forestland	0.00	4.84	79.67	10.19	0.00	0.00	0.00	0.00	0.00	5.30
Grassland	2.87	4.24	84.63	1.34	0.49	0.26	2.37	0.09	0.31	3.40
Water area	0.00	8.49	50.67	31.73	0.75	0.00	0.00	0.00	0.00	8.37
Building site	0.00	10.93	34.89	7.51	36.35	0.00	0.00	0.00	0.00	10.33
Flowing blowout	0.00	0.18	32.46	0.00	0.00	6.72	7.76	26.55	11.80	14.53
Flowing depositional region	0.43	0.35	36.49	0.00	0.00	1.45	6.49	12.93	27.60	14.25
Fixed blowout	0.00	6.43	59.49	34.08	0.00	0.00	0.00	0.00	0.00	0.00
Fixed depositional region	0.00	6.34	92.89	0.00	0.71	0.00	0.06	0.00	0.00	0.00
Flat sandy land	2.99	0.63	58.24	2.04	0.06	1.96	2.27	2.82	3.92	25.07

4.2. Blowout evolution prediction

With the land coverage pattern in 2009 set as the initial state, the CA-Markov model was used to predict future land coverage patterns (Fig.2 and Fig.3). From 2012 to 2020, land use patterns were predicted to maintain the present situation, meaning that grasslands will decrease and the amplitude will dwindle to 4.02%. The areas of other land coverage types will increase; the amplitudes of flowing blowouts and depositional regions will increase by 27.10% and 10.13%, respectively. These rates are less than the present speed. The areas of fixed blowouts and depositional regions will continuously increase; the amplitudes will be 59.04% and 41.44%, respectively. These values indicate that according to the present situation, blowouts will be effectively controlled if the effects of human activities become insignificant.

The simulations must be examined for consistency with actual conditions. Unfortunately, there is no currently available unified evaluation method. Generally, the methods of point-by-point comparison and integral comparison are used. The former method involves an overlay analysis between simulation and actual situation results, comparing calculation accuracies with each point. The latter method not only emphasizes the correctness of a point position, but also considers the entire spatial pattern of the result, such as the Moran I index method (Xia et al., 2007). To determine immediately the accuracy of a simulation, the method of point-by-point comparison was used in the present study. Map algebra calculations with a simulation result graph of 2009 and an interpretation graph of 2009 were completed. The prediction accuracy was 89.02%, which is a good value.

Generally speaking, common forecast models include the remote-sensing geographic information system (Ma, 1996), cellular automata (CA) (Zhou et al., 1999), statistical (Regression Analysis, Markov, Grey System, and so on) (Xu, 2002), and differential-equation dynamic models (Durán et al., 2010). Among them, the Markov Model cannot simulate changes in spatial patterns (Kiira, 1995). While previous studies about CA possesses are mostly concentrated on local interactions at the cellular level, which has certain limitations (Britaldo et al., 2002). Compared with other geographic information system (GIS) and statistical methods, the CA-Markov model is fast, accurate, and real-time (Guan et al., 2011). And compared with the dynamic model, the CA-Markov model is easy to use.

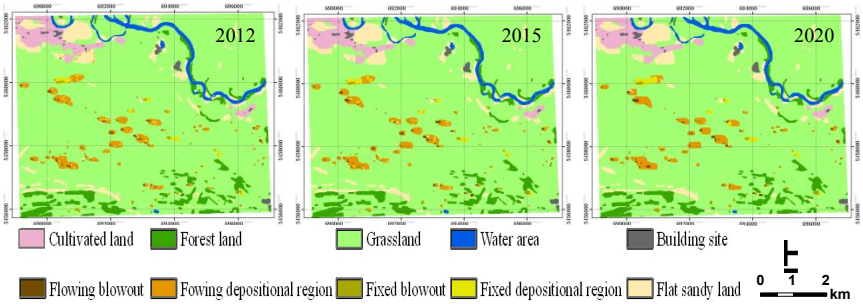

Fig. 2 Land coverage simulation

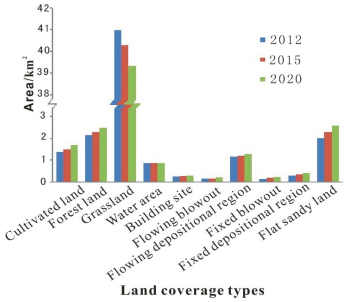

Fig. 3 Future land coverage area

5. Conclusions

Based on 3S technology and long-term series image data, land coverage changes in the Hulun Buir grassland were studied. And the CA-Markov model was used to predict the formation of blowouts in the study region. The following conclusions were drawn.

Each land coverage type in the study region has big amplitude. Grasslands have become the most important recharge sources of other land coverage types in the past 50 years. Forestlands have the highest increased amplitude. The average annual growth rates of the areas of cultivated lands and forestlands are 4.04% and 17.84%. The areas of flowing blowouts and depositional regions show an initial increasing trend, but in the past five years, the areas have decreased. Fixed blowouts and depositional regions have rapidly increased in five years. Grasslands are the main sources of the other land coverage types.

Land coverage pattern from 2012 to 2020 is predicted to maintain the present trend but the development speed will slow down. Grasslands will continue to decrease, and their amplitudes will decrease to 4.02%. The amplitudes of the flowing blowouts and depositional regions will be 27.10% and 10.13%. The areas of fixed blowouts and depositional regions will continue to increase to 59.04% and 41.44%, respectively. This prediction means that blowouts will be controlled if the present natural and human factors are maintained.

6. Acknowledgements

This project is supported by the National Natural Science Foundation of China（NO.41171002）, and National Science and Technology Research during the 12th Five-Year Plan Period (No.2012BAD16B02).

7. References

[1] A. Etter, C. McAlpine, D. Pullar, et.al. Modelling the conversion of Colombian lowland ecosystems since 1940: Drivers, patterns and rates. *Journal of Environmental Management*, 2006, 79: 74-87.

[2] A. Kiira. Simulating vegetation dynamics and land use in a mire landscape using a Markov model. *Landscape and Urban Planning*, 1995, 31(1):129-142.

[3] A. Veldkamp, EF. Lambin. Predicting land-use change. Agriculture. *Ecosystems and Environment*, 2001, 85: 1-6.

[4] ACW. Baas, JM. Nield. Ecogeomorphic state variables and phase-space construction for quantifying the evolution of vegetated aeolian landscapes. *Earth Surface Processes and Landforms*, 2010, 35, 717-731.

[5] CH. Zhou, ZL. Sun, YC. Xie. *Geographical cellular automata research*. Beijing: Science press, 1999.

[6] DN. Xiao, Y. Zhao, ZW. Sun. Changes in spatial pattern of west suburb landscape in Shenyang City. Beijing: *Chinese Forestry Press*, 1991.

[7] EF. Lambin, BL. Turner, H. Geist, S. Agbola, et al. The causes of LU and land-cover change: Moving beyond the myths. *Global Environmental Change*, 2001, 11:261-269.

[8] Guan DJ, Li HF, Inohae T, et al. Modeling urban land use change by the integration of cellular automaton and Markov model. *Ecological Modeling*, 2011, 222:3761-3772.

[9] J. Tang, XG. Wang, SY. Li, et al. The Tendency Forecast on Land Use Landscape Pattern Change in Western Jilin Province Based on CA-Markov Model. Journal of Jilin University (Earth Science Edition), 2010, 40(2):405-411.

[10] J. Wang, YQ. Chen, XM. Shao, et al. Land-use changes and policy dimension driving forces in China: Present, trend and future. *Land Use Policy*, 2012, 29(4):737-749.

[11] JH. Xu. *The mathematical method of modern geography sciences*. Beijing: Higher Education Press, 2002.

[12] L. Xia, JA. Ye, XP. Liu, et al. *Geographical simulation system: cellular automata and Multi-Agent*. Beijing: Science press, 2007.

[13] M. Ainai. Remote sensing information models of geography. *Acta Geographica Sinica*, 1996, 51(3):266-271.

[14] M. Cheema and W. Bastiaanssen. Land use and land cover classification in the irrigated Indus Basin using growth phenology information from satellite data to support water management analysis. *Agricultural water management*, 2010, 97:1541-1552.

[15] O. Durán, EJR. Parteli, HJ. Herrmann. A continuous model for sand dunes: Review, new developments and application to barchan dunes and barchan dune fields. *Earth Surface Processes and Landforms*, 2010, 35: 1591-1600.

[16] PA. Hesp. Foredunes and Blowouts: Initiation, Geomorphology and Dynamics. *Geomorphology*, 2002, 48(1): 245-268.

[17] S. Britaldo, GCC. Soaresflho, LP. Cassio. Dinamica----a stochastic cellular automata model designed to simulate the landscape dynamics in an Amazonian colonization frontier. *Ecological Modeling*, 2002, 154:217-235.